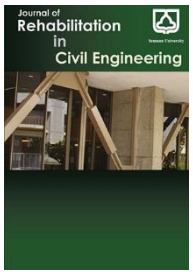

journal homepage: http://civiljournal.semnan.ac.ir/

Study on Rheology Properties, Durability and Microstructure of UHPSCC Contains Garnet, Basalt, and Pozzolan

Alireza Rashno[1], Mohamadreza Adlparvar[1,2*], Mohsen Izadinia[1]

1. Department of Civil Engineering, Najafabad Branch, Islamic Azad University, Najafabad, Iran
2. Department of Civil Engineering, University of Qom, Qom, Iran
Corresponding author: adlparvar@qom.ac.ir

ARTICLE INFO

Article history:
Received: 30 December 2021
Revised: 11 February 2022
Accepted: 19 April 2022

Keywords:
Rheology;
Garnet;
Basalt;
Nano silica;
Durability.

ABSTRACT

This study evaluates the rheology and mechanical properties and durability of concrete, which at the same time has properties of three types of self-compacting concrete (SCC), fiber-reinforced and ultra-high performance. This concrete contains pozzolans, garnet and basalt aggregates, and steel fiber. The purpose of this research is feasibility construction fiber-reinforced ultra-high performance self-compacting concrete (UHPSCC) of durable. Therefore, the required tests on this concrete have been carried out in two steps. The first step is the importance of rheology properties of self-compacting concrete, containing the tests of fresh concrete including slump flow, V-funnel test, and L-box test. The second step involves tests related to the determination of hardened concrete properties divided into two parts. The first part corresponds to the mechanical properties test, including compressive strength, and the second part pertains to durability tests (surface water absorption, surface electrical resistivity and RCMT) and microstructural test, including Scanning Electron Microscopy. The above tests show that this type of concrete has rheology properties in the acceptable range EFNARC, ultra-high compressive strength, negligible surface water absorption, minimal chlorine ion migration coefficient, and very high-level electrical resistance has this type of concrete in the ultra-high concrete cluster.

1. Introduction

SCC is a particular type of concrete that takes the shape of a mold under the influence of its weight flows and usually does not require leveling[1–3]. One of the critical features of SCC is its rheological properties which have been able to solve the pumping

How to cite this article:
Rashno, A., Adlparvar, M., Izadinia, M. (2023). Study on Rheology Properties, Durability and Microstructure of UHPSCC Contains Garnet, Basalt, and Pozzolan. Journal of Rehabilitation in Civil Engineering, 11(1), 96-110
https://doi.org/10.22075/JRCE.2022.25651.1584

and compaction problem[4]. When mixing ordinary concrete and SCC in a fresh state, care must ensure proper bonding between the two layers[5, 6]. A new type and class of concrete produce UHPC with excellent durability and mechanical properties[7–10]. One of the reasons for using chemical additives is to maintain the interaction of components and improve the rheological properties of concrete[11–13]. Nowadays, UHPC is expanding and attracting interest in its usage because of such advantages as compressive strength, high durability, and low permeability[14]. Adding micro silica until the 10% to the Performance of High Strength Concrete increases the compressive strength[15]. In a study, mechanical properties of fiber SCC have been addressed, and three types of fiber were used; results indicated that SCC with different fibers had different mechanical properties[16]. In UHPC, if the value of the binder is less than a specific rate, the rheology and properties will be negatively affected[17]. When fiber is added to UHPC, mechanical properties are considerably enhanced. Various fibers can improve different properties of UHPC[18]. The fiber added to UHPC may result in increased porosity and decreased rheological properties[19, 20]. In the past, the rheology and flowability of different cement composites were studied and resulted in several tests and techniques to investigate fresh concrete properties[21–24]. Yahia et al. investigated the rheological behavior of UHPC[25, 26]. Fiber-reinforced concrete hurts concrete workability while improving the mechanical properties of concrete[27]. UHPFRC uses chemical additives, has good workability, excellent mechanical properties, and high durability[28]. Adding fibers to UHPC improves its mechanical properties significantly[29].

The behavior of fiber-reinforced ultra-high performance self-compacting concrete (UHPSCC) is different from ordinary concrete, and more studies should be done on its properties. So far, few studies have been conducted on UHPSSC consisting of garnet and basalt aggregates and nanosilica, microsilica, and fly ash as well as steel fiber. In this paper, the rheological and mechanical properties, durability, and microstructure of UHPSCC have been reviewed Experimental.

2. Materials

The fine and coarse aggregates (garnet and basalt) were consumed in the standard range of ASTM, and for fine aggregates (sand), the softness module was 2.17 mm. The cement used in concrete samples is Portland cement type 1-525, conforming to ASTM C 150. Nano silica was used in the research with a purity of 99.99%, according to ASTM C 1240. The size of 98% used micro silica in this paper is less than 45 microns conforming to ASTM C 1240. The fly ash conforms to ASTM C 618, and it

consists of 100% class F with grains smaller than 10 microns and an average of 3 microns. A superplasticizer based on polycarboxylic ether has been used in constructing the mixtures. Chemical pozzolanic compounds are presented in Table 1.

Table 1. Pozzolanic materials used and their chemical composition

	CaO	MgO	SO_2	AL_2O_3	Fe_2O_3	Na_2O	K_2O	Cl^-	LOI	SiO_2	ZRO_2
Nanosilica	-	-	-	0.079	-	0.46	-	-	0.2	99.9	-
Fly ash	4.17	2.13	1.06	24.23	6.54	0.88	6.15	0.0205	3.55	49.68	-
Microsilica	0.48	0.12	-	0.25	0.15	-	-	-	-	96	3
Cement	63.56	2.23	2.41	4.83	3.37	0.34	0.52	-	2.1	20.6	-

Specifications superplasticizer used in table 2, the steel fiber used in table 3 and figure 1, the mechanical specifications and the chemical compounds of aggregates are expressed in tables 4 and 5.

Table 2. Specifications for superplasticizer used.

PH	appearance	Special weight 10^{-3} ×(gr/mm^3)	Structure	Ion chlorine
6.6	Pale brown liquid	1.06 to 1.08 in 20 ^oC	Specifications	-

Table 3. Specifications of steel fiber used.

Special weight 10^{-3} ×(gr/mm^3)	Diameter (mm)	Tensile strength (MPa)	Length (mm)
7.8	0.8	1000	35

Fig. 1. Used steel fiber.

Table 4. Mechanical specifications of aggregates used

Materials	Special weight 10^{-3} ×(gr/mm^3)	Water absorption percentage
Sand	2.5	2.8
Garnet	3.6	0.8
Basalt	2.7	2

Table 5. Chemical compounds of aggregates used.

	MgO	CaO	Al_2O_3	TIO_2	MNO	Fe_2O_3	SiO_2	$Fe_2O_3 + FeO$
Garnet	6.1	2	20.6	-	0.6	-	37.2	33.2
Basalt	3.703	8.516	17.39	0.673	-	11.80	50.5	-

3. Construction method

Different models can be used for the particle packing of concrete. The fundamental work of Fuller and Thomsen showed that the packing of concrete aggregates is affecting the properties of the produced concrete[30]. Based on the investigation of Fuller and Thompson a minimal porosity can be theoretically achieved by an optimal particle size distribution (PSD) of all the applied particle materials in the mix as per empirical equation 1 below:

$$P(D) = (\frac{D}{D_{\max}})^q \quad (1)$$

where P(D) is a fraction of the total solids being smaller than size D, D is the particle size (μm), D_{max} is the maximum particle size (μm) and q is the distribution modulus.

However, in the above empirical equation, the minimum particle size is not incorporated, while in reality there must be a finite lower size limit. The most-used particle packing model was originally developed by Andreasen and Andreasen[31]. The model provides an equation that represents the optimal partical size distribution based on the physical characteristics of the constituents; the density and strength of a mixture will theoretically be higher the closer the actual particle size distribution curve is the the optimal curve. this model is shown in Equation 2.

$$P(D) = \frac{D^q - D^q_{\min}}{D^q_{\max} - D^q_{\min}} \quad (2)$$

where D_{min} = minimum particle size in the mix; and all the other parameters are defined previously. A distribution modulus q of 0.25 was considered for the particle packing analysis in this study, based on previous researchers[32–34]. Fig 2 shows the particle size distribution of raw materials.

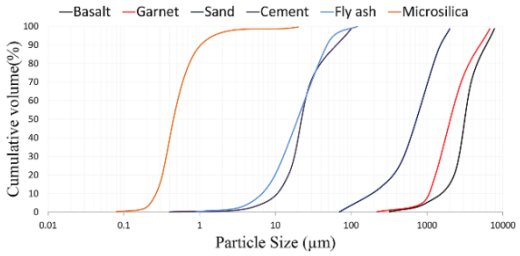

Fig. 2. Particle size distribution (PSD) of raw materials.

Considering the purpose is to construct the fiber-reinforced ultra-high performance self-compacting concrete, in addition to its high resistance and the durability properties of this type of concrete is also important and according to the past research and experimental experiments, the amount of binder (total cementitious materials), 630 kg/m^3 in all mixed designs have been considered fixed[35, 36]. The mixing design of ultra-high performance self-compacting concrete, it has been named (UHPSCC) and has been presented as control concrete and expressed in Table 6.

Table 6. The mixed design of control ultra-high performance self-compacting concrete (kg/m^3).

Mix	Basalt	Garnet	Sand	Cement	Fly ash	Superplasticizer	Microsilica	W/B
UHPSCC(C)	525	525	700	472	94.5	10.1	63.5	2.5

In this paper, the amounts of garnet and basalt aggregates, micro silica, fly ash, and W/B have been regarded as constant in UHPSCC. Consumption of fly ash and micro silica, respectively, are 15% and 10% by weight of cement[37]. As the amounts of nanosilica and steel fiber increased, cement consumption decreased. Nanosilica with 1, 1.5, 2 percent of the weight of cementitious materials[38] and steel fiber with 1, 1.5, 2, 2.5, and 3 percent of the volumetric cementitious materials were added to the control concrete (C).

4. Experimental program and discussion

4.1. Rheological properties

After the material was mixed in the mixer and before the fresh concrete was cast in the form, tests should be conducted to determine the efficiency of the concrete on the fresh concrete. The flow velocity of the self-compacting concrete in form depends on its viscosity. The self-compacting concrete should have four properties: the ability to fill the form by just its weight, resist the grains

segregation, pass the bar without grains segregation, and finally have the appropriate finished surface. To achieve these properties, codes have proposed experiments, including the slump flow diameter, the slump flow time, the L-box, and V-funnel flow time. Suggestions and restrictions are outlined in the codes in the case of the minimum efficiency required to reach the above four attributes. The experiment of slump flow diameter is a typical method to determine the properties related to the fluidity of fresh concrete at a horizontal level with no obstacles. The slump flow time (T50) experiment is a criterion to determine the viscosity amount of self-compacting concrete (SCC).

Fig. 3. Slump flow of UHPSCC.

The experiment of L- box includes round bars to determine the ability to pass and disperse in the surrounded SCC. The V-funnel experiment is used to assess the dough viscosity and concrete mortar workability. The results rheology properties of different designs are presented in figure 4 and acceptance criteria of SCC suggested by EFNARC in table 7.

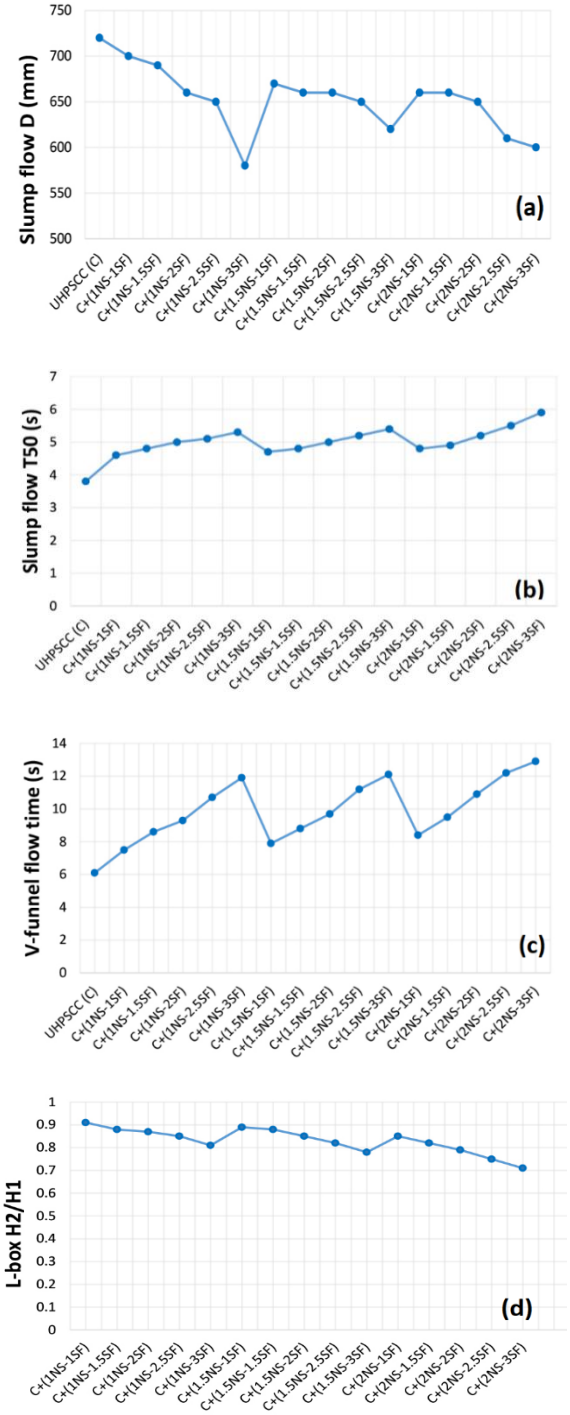

Fig. 4. The rheology properties of UHPSCC: (a) Slump flow D, (b) Slump flow T(50), (c)V-funnel, (d) L-box.

Table 7. Acceptance criteria of SCC suggested by EFNARC

	Slump flow D (mm)	Slump flow T50 (s)	V-funnel flow time (s)	L-box H2/H1
Acceptance criteria of SCC suggested by EFNARC[1, 39]	**650-800**	**2-5**	**6-12**	**0.8-1**

In Figure 4, the names and plans are as follows:

UHPSCC (C): Ultra-High Performance Self-Compacting Concrete

NS: NanoSilica

SF: Steel Fiber

C+(2NS-1SF): UHPSCC+2% weight cementitious materials nanosilica and 1%

volumetric cementitious materials of steel fiber. According to Figure 4 results of fresh concrete experiments showed that due to pozzolanic materials in the concrete (C), the parameters related to fresh concrete are put in the acceptable range of EFNARC[1, 39, 40]. The increased amounts of nanosilica and steel fiber lead to the decreased concrete efficiency so that 3% steel fiber in the experiment of slump flow diameter, 2.5% steel fiber in the experiment of slump flow T50, and 3% steel fiber in the V- funnel experiment led to exit from the accepted range. In the V-funnel experiment, it is obvious that steel fiber has a negative effect on fresh concrete properties, and nanosilica decreases the efficiency and increases fresh concrete viscosity. Given that nanosilica particles absorb more water, the slump flow diameter decreased. Adding nanosilica to the plan, V- funnel experiment time and T50 slump flow have increased. A study by Teng et al[19] Shows that adding 1 to 3% steel fiber to the UHPC increased the V-funnel flow time, which in the present study also showed a similar result as increasing the amount of steel fiber. The increased amounts of nanosilica and steel fiber in the plans have decreased the H2/H1 ratio in the L-box experiment.

4.2. Mechanical properties and durability

4.2.1. Compressive strength test

The compressive strength test has been done as the most important representative of mechanical behavior of concrete on cube samples based on BS EN 12390-3:2019[41]. In this experiment, 100 mm cube samples were used.

Fig. 5. Compressive strength of UHPSCC.

The results of the UHPSCC compressive strength test have been presented in Fig.6 and show the very high compressive strength of this concrete type. One of the reasons for high compressive strength is the aggregates used in the concrete in addition to the pozzolanic materials in the mixture. Considering the specific surface area high of

nanosilica, reactivity is so high that it accelerates the hydration process and affects high compressive strength. Microsilica accelerates the hydration and compressive strength. But this acceleration is less than nanosilica. Nanosilica acceleration is more at low ages, whereas it is less than micro silica at high ages. So using nanosilica and micro silica simultaneously increases the compressive strength of concrete at low ages compared to micro silica. The plasticizer can disconnect the clods through being absorbed by the cement particles surface, especially ca^{2+} ions on nanosilica particles surface, and as a result, mechanical properties are enhanced. Also, using a combination of nanosilica and micro silica decreases the use of plasticizers compared to the mixtures consisting of only nanosilica. UHPSCC is a brittle material, while the addition of steel fibers to UHPSCC improves the brittle behavior of concrete and changes its fracture mode. Steel fibers resist crack propagation and positively affect the mechanical properties of concrete in all fracture modes. Fine and spherical particles in the shape of fly ash reduce the amount of water in the concrete mix and improve the rheology of UHPSCC, reducing the possibility of the phenomenon of water separation of aggregates in concrete. The reaction of fly ash with calcium hydroxide $Ca(OH)_2$ resulting from dewatering of cement and production of C-S-H causes it to fill concrete pores and increases the durability of concrete against aggressive environments.

Garnet and basalt aggregates are elements resulting in compact and strength. Iron oxide in the garnet aggregates reduces intra-grains failure. Garnet and basalt aggregates have increased the compressive strength and concrete strength. According to Fig.5, a 12% difference has been observed between the compressive strength of control concrete and concrete with 1% nanosilica and 1% steel fiber. The increased percentage of nanosilica and steel fiber increased the compressive strength so that the percentage of increased compressive strength of concrete and the most resistant concrete reached more than 50%. The plan involves 2% nanosilica and 2% steel fiber and has the most compressive strength; it increases the compressive strength to 34% as compared to the treatment involving 1% nanosilica and 1% steel fiber. In the treatments involving 2% nanosilica, compressive strength decreased while adding 2% steel fiber. It seems that the C+(2NS-2SF) treatment is an optimized one regarding compressive strength. A study conducted in 2019 shows that a 2% increase in steel fibers and a 10 to 20% increase in silica fume to UHPC has increased the compressive strength to 120[20]; that shows that the UHPC studied in the present study has a higher compressive strength.

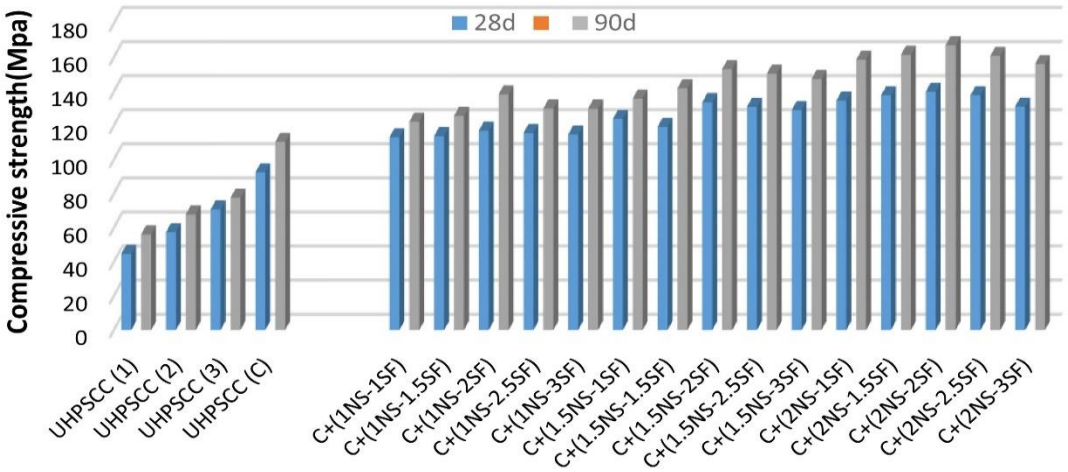

Fig. 6. Compressive strength of fiber-reinforced UHPSCC.

4.2.2. Surface water absorption test

The surface water absorption of concrete is one of the determinants in concrete durability. To perform this experiment, a cubic specimen has been used. The specimens have been tested according to BS1881part208 standard[42]. In this experiment, the amount of poured water adsorption on the horizontal surface of the concrete specimen is where there is no few heights of water to apply pressure and by applying the water pressure of 200 mm on a certain horizontal surface of the concrete, the rate of surface water uptake is measured at a different time. The results and the percentage of surface water absorption at 1, 10, 30, and 60 minutes of different designs are presented in figure 7.

The surface water absorption test results indicate that the presence of aggregates with low water absorption, particularly the garnet aggregate in the specimens of the experiment, has reduced the water absorption of the concrete designs and has placed this concrete in more favorable conditions compared with conventional structural concretes. Also, by adding 1% of silica nanoparticles to the control concrete, its surface water absorption is reduced by 27%. In the designs containing nanosilica and steel fiber, the percentage of steel fiber used in surface water absorption has increased. This increase is less developed by adding nanosilica to the design. In designs containing 1% of steel fiber, 1, 1.5, and 2% of the weight of cement materials of nanosilica, respectively have 0.022, 0.015, and 0.009, which is the lowest amount of surface water absorption related to the C+(2NS-1SF) design. The above results show the reduction of surface water absorption of the designs by increasing the amount of nanosilica in each design. The existence of pozzolans in the concrete design has decreased the interstices and pores. It has led to less water absorption, which indicates the optimal surface quality of the concrete and increases the resistance.

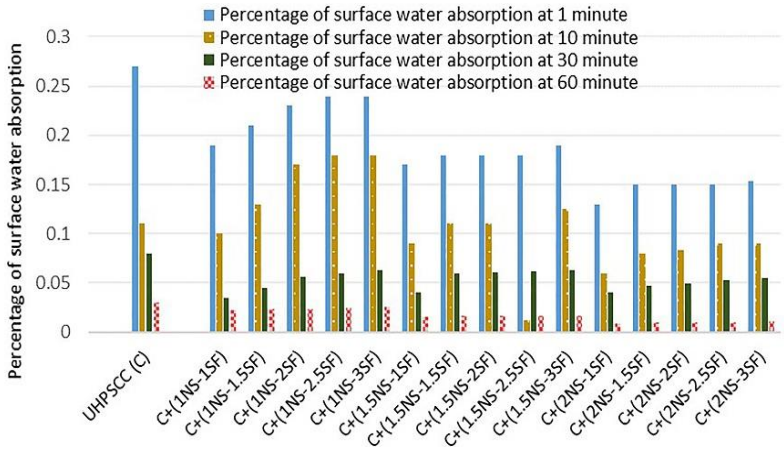

Fig. 7. Comparison of surface water absorption percentage of UHPSCC at times of 1, 10, 30, and 60 minutes.

4.2.3. Surface electrical resistivity test

Ions that have penetrated the concrete environment move through the pores in the concrete structure. Due to the movement of ions inside the concrete environment, the concrete has electrical conductivity. There is a connection between electrical resistivity and the permeability of the concrete and ambient conditions. The higher the permeability of the concrete, the more easily and faster the ions can penetrate the concrete environment, so the electrical resistivity of the concrete is reduced, and the concrete is low resistant to the penetration of the chlorine ion and corrosion. In other words, the longer the electrical resistivity of the concrete is higher, the more resistant of concrete to corrosion.

This parametric test is designed to evaluate the possible corrosion rate of reinforced concrete specimens in the chloride attack, where cylindrical specimens were constructed with dimensions 100×200 mm and were tested at 28 and 90 days. In this method, the Wenner probe has been used with four electrodes, which are linear with equal distance and length of 38 mm. The electrodes' contact with the surface of the saturation concrete specimen is easily established through the wet sponges placed on the electrodes. In two external electrodes, the current of electricity is established at a given frequency by a feeding source, and voltage is measured in two internal electrodes. The Wenner probe's peak voltage is to the maximum of 38 volts and at 40 Hz frequency.

Figure 8 shows the results of a surface electrical resistivity test at 28 and 90 days. The presence of aluminum compounds in the aggregate and fly ash caused a high rise in the surface electrical resistivity of this type of concrete. The increase of steel fiber in control concrete design reduces the surface electrical resistivity. The lowest amount of the above resistance is related to a design that contains 1% nanosilica and 3% steel fiber. The reduction rate of the surface electrical resistivity of design C+(1NS-3SF) at the age of 90 days compared to the control concrete (C) is 47% due to steel fiber present in the design. The highest surface electrical resistivity is related to the control concrete. After that, among the designs containing nanosilica and steel fiber, the highest surface

electrical resistivity is related to the C+(2NS-SF) design.

The results show the effect of pozzolans in the increase of surface electrical resistivity in the fiber-reinforced ultra-high performance self-compacting concrete, especially at higher ages.

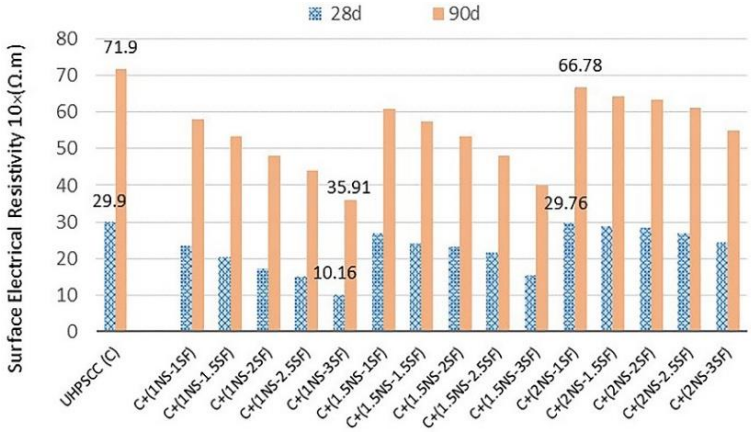

Fig. 8. The results of the concrete surface electrical resistivity test of UHPSCC

4.2.4. Rapid Chloride Migration Testing (RCMT)

One of the tests widely used to measure the diffusion coefficient of chloride ions is the rapid chloride migration testing. The experiment was carried out based on the NT BUILD-492 standard[43]. To perform this experiment, a cylindrical specimen of 100×200 mm is used at each age, which, in the form of three cylindrical section of 50×100 mm, is cut out. The experiment was carried out at the ages of 28 and 90 days.

After being saturated with water, the specimens were placed inside the rubbery sheath, and their perimeter surface was isolated. Naoh solution was poured with a concentration of 0.3 normal inside the rubbery sheath, and it is in contact with the upper section of the concrete specimen. The set prepared inside the container containing NaCl solution is placed with a concentration of 10% so that the bottom section of the specimen is in contact with NaCl solution.

For the start of the experiment, electrodes are attached to the direct current generator device. At the start of the applied voltage, is set 30V, and the proper voltage is modified according to the initial flow of pass. The temperature of hydroxide sodium solution at the first and end of the experiment is recorded. After the experiment's time passes and applies a voltage across the specified time range, the extinct device and specimen will go out of the rubbery sheath. Then the specimen was split into two halves, and the $AgNO_3$ solution (0.1 molars) is sprayed on a broken new surface and the penetration depth of chloride ion is determined by measuring the depth of the data color change area. Finally, the chloride ion migration coefficient is calculated in an unstable condition of Equation 3.

$$D_{nssm} = \frac{0.0239(273+T)L}{(U-2)t}(X_d - 0.0238)\sqrt{\frac{(237+T)X_d}{(U-2)}} \quad (3)$$

Where D_{nssm} is the non-steady-state migration coefficient $\times 10^{-12}$ in m^2/s, U is the absolute value of the voltage applied in V, T is the average value of the initial and final temperatures in the anolyte solution in ˚C, L is the thickness of the specimen in mm, X_d is the average value of the penetration depths in mm, t is the test duration in an hour. Figure 8 show the results of a rapid chloride migration testing (RCMT) at 28 and 90 days. Figure 9 shows the lowest migration coefficient of the chloride ion associated with the UHPC (C) design. At the same time, increased nanosilica and steel fiber to the control design have increased the penetration depth average of chlorine ions. This increase has grown more by adding a higher percentage of fiber to the design, So that this coefficient at the age of 90 d in the plan C+(1NS-1SF) and C+(1NS-3SF) compared to UHPSCC (C) has increased more than 2 and 5 fold, respectively. The highest chloride ion migration coefficient is related to the C+(1NS-3SF) design. As the amount of nanosilica increases to the design, this growth has decreased and decreased the migration coefficient increases

of the chlorine ion. The chloride ion migration coefficient has increased with the increased percentage of fiber to specimens, and the highest is related to the C+(1NS-3SF) design. As the amount of nanosilica increases to the design, this growth has decreased and decreased the migration coefficient increases of the chlorine ion. For example, this coefficient shows a 39% decrease at the age of 90 d in C+(2NS-1SF) compared to C+(1NS-1SF).

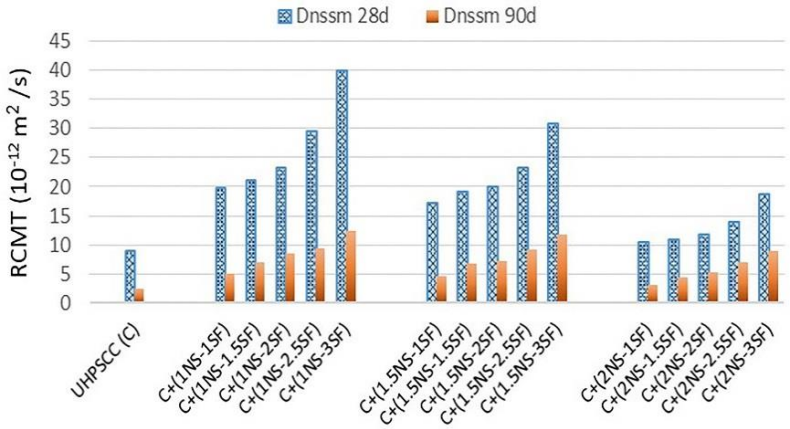

Fig. 9. The results of the RCMT of UHPSCC

4.3. Scanning electron microscopic (SEM)

The SEM images are shown in figure 10. In order to closer investigate the microstructure of the cement matrix and the transfer region, needs to include the scales are different in these SEM images. 250 scale (figure 10(a)) is used to detect different phases, and 5000 and 20000 scales (figure 10(b)) are used to examine the transition area and also the impact of the presence of pozzolans fibers and other consumables materials on this area.

The study of the microstructure of concrete in SEM images shows that the nanosilica particles make the pores smaller and prevent the micro cracks, thus increasing the resistance of these specimens with the presence of nanosilica. The type, shape, texture of the grains surface and the main

minerals of the aggregates resulted in reduced porosity and increased the material's cohesion to cement paste. Nanosilica and fly ash are caused by the pozzolanic reaction of the generated adhesive material. These materials are reacted with calcium hydroxide, a non-adhesive material with a high concentration in the intersurface transport zone (ITZ). This reaction produces silicate hydrate calcium gel, which reduces the porosity and increases the graft strength of the cement paste and the aggregate. In effect, the addition of nanosilica to cement particles gives the formation of $H_2Sio_4^{2-}$ and it starts to react with $Ca^{2+}$and is produced the extra calcium-silicate-hydrate (C-S-H). The formation of a large number of these particles has accelerated hydration time. The amorphous mass is integrated and attached at all surfaces of failure. Fine nanoparticles have caused thecrevices bridging in the joint surface between the aggregate and the cement matrix. Therefore, the aggregate used causes an increase in compressibility to reduce segregation, and shrinkage, thus increasing the compressive strength and durability and causing a reduction in permeability.

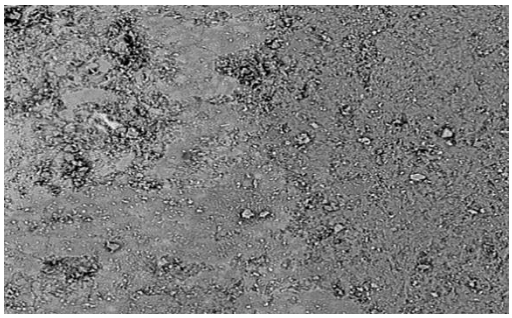

(a)

(b)

Fig. 10. (a, b) SEM images of UHPSCC.

5. Conclusions

This experimental study is designed to investigate the rheology properties, mechanical properties, and durability of concrete that simultaneously characterize the properties of three types of self-compacting concrete, ultra-high performance concrete, and fiber-reinforced concrete. This fiber-reinforced ultra-high performance self-compacting concrete includes aggregates of garnet and basalt, pozzolanic materials (micro silica, nanoparticles, and fly ash), as well as steel fiber. This research first examines the rheology properties of different designs with different amounts of steel fiber and nanosilica. Compressive strength, surface water absorption, surface electrical resistivity, Rapid Chloride Migration Testing (RCMT), SEM were investigated. The results of this study are presented as follows:

- Due to the existence of micro silica and fly ash in the UHPSCC, the rheological properties were put in the acceptance range of EFNARC. The effect of adding nanosilica and steel fiber simultaneously to the mix up to 2% had a positive impact on the rheological properties of the desired concrete but the increase of more than 2% in steel fiber took the fresh concrete rheological properties out of the acceptance range EFNARC.

-The aggregates garnet and basalt have compounds that make them harder and more resistant. The intergranular fracture due to increased adhesion between the cement and aggregates has been decreased, increasing the compressive strength of the concrete. The addition of nanosilica particles and steel fiber has improved the compressive strength of fiber-reinforced ultra-high performance self-compacting concrete. Porosity due to pozzolanic reaction reduces the available calcium hydroxide in concrete, and as well as with the improvement of the transition region in concrete, will increase the compressive strength.

-Pozzolanic reaction led to the production of adhesives and reacted with calcium hydroxide as a non-adhesive and high concentration in ITZ. The product of this reaction is a calcium-silicate-hydrate gel (C-S-H), increasing the adhesion, decreasing capillary and porous cavities, and condensing ITZ in UHPC. It reduces surface water absorption and rapid chloride migration testing (RCMT) and enhances surface electrical resistivity.

REFERENCES

[1] Bibm, C.; ERMCO, E. (2005). EFNARC: The European Guidelines for Self Compacting Concrete, Specification, Production and Use, Vol. 63

[2] Lachemi, M.; Hossain, K. M. A.; Lambros, V.; Bouzoubaa, N. (2003). Development of cost-effective self-consolidating concrete incorporating fly ash, slag cement, or viscosity-modifying admixtures, Materials Journal, Vol. 100, No. 5, 419–425

[3] Okamura, H.; Ouchi, M. (1998). Self-compacting high performance concrete, Progress in Structural Engineering and Materials, Vol. 1, No. 4, 378–383

[4] Varela, H.; Barluenga, G.; Palomar, I. (2020). Influence of nanoclays on flowability and rheology of SCC pastes, Construction and Building Materials, Vol. 243, 118285

[5] Megid, W. A.; Khayat, K. H. (2019). Effect of structural buildup at rest of self-consolidating concrete on mechanical and transport properties of multilayer casting, Construction and Building Materials, Vol. 196, 626–636

[6] Vos, M.; Torres, E.; Alrashidi, R. S.; Riding, K.; Hamilton, T. (2019). Evaluation of bond strength of joints in hybrid uhpc and scc members, International Interactive Symposium on Ultra-High Performance Concrete (Vol. 2), Iowa State University Digital Press

[7] Habel, K.; Viviani, M.; Denarié, E.; Brühwiler, E. (2006). Development of the mechanical properties of an ultra-high performance fiber reinforced concrete (UHPFRC), Cement and Concrete Research, Vol. 36, No. 7, 1362–1370

[8] Wille, K.; Naaman, A. E.; Parra-Montesinos, G. J. (2011). Ultra-High Performance Concrete with Compressive Strength Exceeding 150 MPa (22 ksi): A Simpler Way., ACI Materials Journal, Vol. 108, No. 1

[9] de Larrard, F.; Sedran, T. (1994). Optimization of ultra-high-performance concrete by the use of a packing model, Cement and Concrete Research, Vol. 24, No. 6, 997–1009

[10] Meng, W.; Valipour, M.; Khayat, K. H. (2017). Optimization and performance of cost-effective ultra-high performance concrete, Materials and Structures, Vol. 50, No. 1, 1–16

[11] Kovler, K.; Roussel, N. (2011). Properties of fresh and hardened concrete, Cement and Concrete Research, Vol. 41, No. 7, 775–792

[12] Mikanovic, N.; Jolicoeur, C. (2008). Influence of superplasticizers on the rheology and stability of limestone and cement pastes, Cement and Concrete Research, Vol. 38, No. 7, 907–919

[13] Jiao, D.; Shi, C.; Yuan, Q.; An, X.; Liu, Y.; Li, H. (2017). Effect of constituents on

rheological properties of fresh concrete-A review, Cement and Concrete Composites, Vol. 83, 146–159

[14] Khaksefidi, S.; Ghalehnovi, M. (2020). Effect of Reinforcement Type on the Tension Stiffening Model of Ultra - High Performance Concrete (UHPC), Vol. 3, 72–86. doi:10.22075/JRCE.2020.19420.1368

[15] Ahmadi, N.; Yazdandoust, M.; Yazdani, M. (2021). Simultaneous Effect of Aggregate and Cement Matrix on the Performance of High Strength Concrete, Journal of Rehabilitation in Civil Engineering, 26–39

[16] Falahtabar, M.; Tavakoli, H. R. (2018). Estimation of Mechanical and Durability Properties of Self - Compacting Concrete with Fibers Using Ultrasonic Pulse Velocity, Vol. 2, 43–53. doi:10.22075/JRCE.2018.798.1099

[17] Ding, M.; Yu, R.; Feng, Y.; Wang, S.; Zhou, F.; Shui, Z.; Gao, X.; He, Y.; Chen, L. (2021). Possibility and advantages of producing an ultra-high performance concrete (UHPC) with ultra-low cement content, Construction and Building Materials, Vol. 273, 122023. doi:10.1016/j.conbuildmat.2020.122023

[18] Huang, H.; Gao, X.; Teng, L. (2021). Fiber alignment and its effect on mechanical properties of UHPC : An overview, Construction and Building Materials, Vol. 296, 123741. doi:10.1016/j.conbuildmat.2021.123741

[19] Teng, L.; Meng, W.; Khayat, K. H. (2020). Cement and Concrete Research Rheology control of ultra-high-performance concrete made with different fiber contents, Cement and Concrete Research, Vol. 138, No. July, 106222. doi:10.1016/j.cemconres.2020.106222

[20] Wu, Z.; Khayat, K. H.; Shi, C. (2019). Changes in rheology and mechanical properties of ultra-high performance concrete with silica fume content, Cement and Concrete Research, Vol. 123, No. October 2018, 105786. doi:10.1016/j.cemconres.2019.105786

[21] Roussel, N.; Coussot, P. (2005). "Fifty-cent rheometer" for yield stress measurements: from slump to spreading flow, Journal of Rheology, Vol. 49, No. 3, 705–718

[22] Ferrara, L.; Cremonesi, M.; Tregger, N.; Frangi, A.; Shah, S. P. (2012). On the identification of rheological properties of cement suspensions: Rheometry, Computational Fluid Dynamics modeling and field test measurements, Cement and Concrete Research, Vol. 42, No. 8, 1134–1146

[23] Choi, M. S.; Lee, J. S.; Ryu, K. S.; Koh, K.-T.; Kwon, S. H. (2016). Estimation of rheological properties of UHPC using mini slump test, Construction and Building Materials, Vol. 106, 632–639

[24] Jalal, M.; Teimortashlu, E.; Grasley, Z. (2019). Performance-based design and optimization of rheological and strength properties of self-compacting cement composite incorporating micro/nano admixtures, Composites Part B: Engineering, Vol. 163, 497–510

[25] Yahia, A.; Khayat, K. H. (2003). Applicability of rheological models to high-performance grouts containing supplementary cementitious materials and viscosity enhancing admixture, Materials and Structures, Vol. 36, No. 6, 402–412

[26] Yahia, A. (2011). Shear-thickening behavior of high-performance cement grouts—Influencing mix-design parameters, Cement and Concrete Research, Vol. 41, No. 3, 230–235

[27] Gerland, F.; Schleiting, M.; Schomberg, T.; Wünsch, O.; Wetzel, A.; Middendorf, B. (2019). The effect of fiber geometry and concentration on the flow properties of UHPC, Rheology and Processing of Construction Materials, Springer, 482–490

[28] Matos, A. M.; Nunes, S.; Costa, C.; Barroso-Aguiar, J. L. (2019). Characterization of non-proprietary UHPC for use in rehabilitation/strengthening applications, Rheology and Processing of Construction Materials, Springer, 552–559

[29] Yu, R.; Van Onna, D. V; Spiesz, P.; Yu, Q. L.; Brouwers, H. J. H. (2016). Development of ultra-lightweight fibre reinforced concrete applying expanded waste glass, Journal of Cleaner Production, Vol. 112, 690–701

[30] Fuller, W. B.; Thompson, S. E. (1907). The laws of proportioning concrete, Transactions of the American Society of Civil Engineers, Vol. 59, No. 2, 67–143

[31] Andreasen, A. H. M. (1930). Über die Beziehung zwischen Kornabstufung und Zwischenraum in Produkten aus losen Körnern (mit einigen Experimenten), Kolloid-Zeitschrift, Vol. 50, No. 3, 217–228

[32] Kurt, A. (2021). Implementation of Ultra-High Performance Concrete in Long-Span Precast Pretensioned Structural Elements for Buildings, North Carolina State University

[33] Alkaysi, M.; El-Tawil, S. (2016). Effects of variations in the mix constituents of ultra high performance concrete (UHPC) on cost and performance, Materials and Structures, Vol. 49, No. 10, 4185–4200

[34] Looney, T.; McDaniel, A.; Volz, J.; Floyd, R. (2019). Development and characterization of ultra-high performance concrete with slag cement for use as bridge joint material, Development, Vol. 1, No. 02

[35] Parichatprecha, R.; Nimityongskul, P. (2009). Analysis of durability of high performance concrete using artificial neural networks, Construction and Building Materials, Vol. 23, No. 2, 910–917

[36] Venkatakrishnaiah, R.; Sakthivel, G. (2015). Bulk utilization of flyash in self compacting concrete, KSCE Journal of Civil Engineering, Vol. 19, No. 7, 2116–2120

[37] Arora, A.; Aguayo, M.; Hansen, H.; Castro, C.; Federspiel, E.; Mobasher, B.; Neithalath, N. (2018). Microstructural packing-and rheology-based binder selection and characterization for Ultra-high Performance Concrete (UHPC), Cement and Concrete Research, Vol. 103, 179–190

[38] Janković, K.; Stanković, S.; Bojović, D.; Stojanović, M.; Antić, L. (2016). The influence of nano-silica and barite aggregate on properties of ultra high performance concrete, Construction and Building Materials, Vol. 126, 147–156

[39] EFNARC, S. (2002). Guidelines for self-compacting concrete, London, UK: Association House, Vol. 32, 34

[40] Concrete, S.-C. (2005). The European guidelines for self-compacting concrete, BIBM, et Al, Vol. 22

[41] BS EN 12390-3:2019 Testing hardened concrete. Compressive strength of test specimens, British Standards Institution - Publication Index | NBS. (2019), 12390

[42] Institution, B. S. (1998). Testing Concrete: Recommendations for the Determination of the Initial Surface Absorption of Concrete, BSI

[43] Build, N. (1999). 492. Concrete, mortar and cement-based repair materials: Chloride migration coefficient from non-steady-state migration experiments, Nordtest Method, Vol. 492, No. 10